

*Article*

## Effect of Filler Metals on Creep Properties of 2.25Cr-1Mo Steel Weld Joints Prepared by GTAW Process

Buntoeng Srikarun<sup>1,a</sup>, Ittiphol Phonpud<sup>2,b</sup>, Prapas Muangjunburee<sup>2,3,c,\*</sup>,  
and Thawatchai Plookphol<sup>3,d</sup>

<sup>1</sup> Department of Mechanical and Robotic Engineering, School of Engineering and Technology, Walailak University, Thasala, Nakhon Si Thammarat 80160, Thailand

<sup>2</sup> Department of Mining and Materials Engineering, Faculty of Engineering, Prince of Songkla University, Hat Yai, Songkhla 90110, Thailand

<sup>3</sup> Center of Excellence in Metal and Materials Engineering, Faculty of Engineering, Prince of Songkla University, Hat Yai, Songkhla 90110, Thailand

E-mail: <sup>a</sup>buntoeng.sr@wu.ac.th, <sup>b</sup>ittiphon31@gmail.com, <sup>c,\*</sup>prapas.m@psu.ac.th (Corresponding author), <sup>d</sup>thawatchai.p@psu.ac.th

**Abstract.** This research aims at comparing creep properties at elevated temperatures obtained on welding 2.25Cr-1Mo steel using gas tungsten arc welding (GTAW) with ER90S-G and ERNiCrMo-3 filler metals. The high temperature accelerated creep rupture test of 2.25Cr-1Mo welded samples was investigated over 139 to 315 MPa stress range at temperatures of 550 °C, 600 °C, and 650 °C. The samples were preheated at 250 °C for 0.5 hours and post-weld heat-treated at 690 °C for 1 hour. The results showed that the accelerated creep rupture lives of lower applied stress specimens were much longer than those of higher applied stress, when both welded materials were tested under same temperature conditions. The service lifetime of the welded materials can be predicted using the extrapolation of the Larson-Miller parameter. Creep surface fractures were investigated using SEM fractography that indicated the weldment fracture modes consisted of dimple ruptures and micro-voids coalescence in the fibrous matrix of the intercritical region of HAZ. Similar high-temperature creeps service lives were found in both welded materials.

**Keywords:** Accelerated creep, creep rupture, 2.25Cr-1Mo steel, GTAW, Larson-Miller parameter.

ENGINEERING JOURNAL Volume 26 Issue 3

Received 17 June 2021

Accepted 8 March 2022

Published 31 March 2022

Online at <https://engj.org/>

DOI:10.4186/ej.2022.26.3.71

## 1. Introduction

In energy generating industries, various types of engineering components are operating at elevated temperatures. To consider the suitable materials used for these components, excellent resistance to high temperatures and corrosion is one of the properties of heat-resistant steel. Metallic materials at elevated temperatures must be considered the time-dependent deformation and fracture behavior in their design [1].

High-temperature steel alloys are widely used in power generating steam plants, fossil power plants, oil refineries, chemical plants, and nuclear power plants. Among those materials, a popular choice is chromium-molybdenum alloy steel because of its excellent resistibility to high temperatures, creep, corrosion, and good weldability at reasonable costs for long-term service lives [2, 3] When it is necessary, the damaged components are usually replaced with the spare parts. However, some damaged parts are repaired by welding as it is more reasonable than replacing with new part or equipment [4].

A common failure cause is a metallic creep which occurs at an elevated temperature for parts under load. [5, 6] Therefore, the material's creep properties are the critical criteria when the suitable alloys for elevated temperatures service are selected. The phenomenon of creep is a slow process at a high temperature, which tends to occur in unrecoverable plastic deformation when the yield strength of tested steel specimen is much higher than the certainly applied stress. The creep curve shows the fundamental phenomenon of the creep mechanism, such as steady-state creep start time, minimum creep rate or steady-state creep, acceleration creep starts time, and rupture time. Therefore, it mainly represents the performance of creep [7].

Inconel 625 is a nickel-based superalloy that proposes high creep resistance at elevated temperatures. Hence, Inconel 625 is widely used in high-temperature power industry applications [8, 9]. The welded samples were tested under accelerated creep test conditions to determine the choice of filler metals for weld repair of chromium-molybdenum steel to avoid failure with a short-term lifetime in engineering components in high-temperature service [10]. In this study, the objective of the present research is to evaluate the creep properties at elevated temperatures of the 2.25Cr-1Mo steel welded using Inconel 625 and 2.25Cr-1Mo as filler metals.

## 2. Material and Methods

The material used in this research were 2.25Cr-1Mo (ASTM A213-T22) base metal steel, AWS ER90S-G, and AWS ERNiCrMo-3 (Inconel 625) filler metal. The chemical compositions of base material and different filler metals are shown in Tables 1, 2, and 3, respectively.

In this research, the size of 2.25Cr-1Mo steel pipe used was outside diameter 60.3 mm, thickness 5.5 mm, and length 100 mm. The weld joint preparation was a single-V groove including groove angle 60, root gap 2 mm,

and root face 1 mm. Before welding, preheating was conducted at 250 °C for 0.5 hours in an electric furnace. The gas tungsten arc welding (GTAW) process with 99.9% purity argon shielding gas was using 2.25Cr-1Mo steel pipe filled by ER90S-G and ERNiCrMo-3 consumable weld metal. The welding parameters used for different filler metals were the same. The welding parameters are welding current 100-105 A, voltage 11-12 V, and welding travel speed 4.4-7.3 cm/min. After welding, post-weld heat treatment (PWHT) was applied 690 °C for 1 hour and cooling after PWHT in a furnace.

The creep test specimen configuration was prepared as followed in Fig. 1 and Table 4. The location of welded at the middle of the specimen and welded size dimension from the middle to each side, approximately 6-8 mm.

Table 1. Chemical Composition of 2.25Cr-1Mo (ASTM A213 T22) Base Metal [11].

Element	Weight (%)	Element	Weight (%)
C	0.13	S	0.035
Si	0.50	Cr	2.25
Mn	0.45	Mo	1.00
P	0.035	Fe	Bal.

Table 2. Chemical Composition of AWS A5.28 ER90S-G Filler Metal [12].

Element	Weight (%)	Element	Weight (%)
C	0.11	Cr	2.29
Si	0.36	Mo	1.07
Mn	0.70	Cu	0.15
Ni	0.04	Fe	Bal.

Table 3. Chemical Composition of AWS A5.14 ERNiCrMo-3 (Inconel 625) Filler Metal [13].

Element	Weight (%)	Element	Weight (%)
C	0.01	Cr	22.1
Mn	0.12	Mo	8.8
Ti	0.18	Nb	3.78
Ni	64.2	Fe	Bal.

Figure 2. presents creep test machine and its accessories equipment. The creep specimen was loaded into the pin-type grips and pull rod assembly supported by a setup jig. The specimen load train assembly was loaded into the furnace retort chamber in the middle of furnace. The total applied force exerted on the cross-section area of the specimen gage section determined the applied stress value, required for each creep test. Total applied force was the sum of the weights from the load train. Once vertical axial alignment of the load train was obtained, the LVDT extensometer was attached to the lower pull rod assembly with recording input to PC computer data acquisition system (DAQ) for logging extensometer transducer output. The specimen temperature profile was maintained within  $\pm 3$  °C of the desired test temperature during testing. All the samples were tested until fracture.

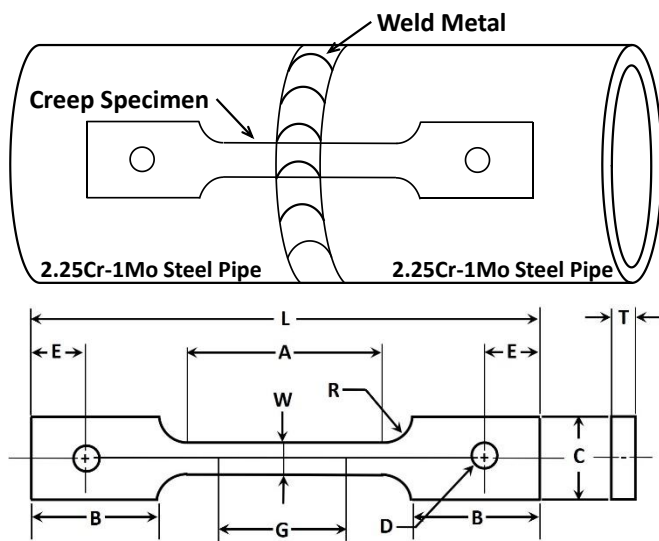


Fig. 1. Creep test specimen [14].

Table 4. The Dimension of Creep Specimen.

Symbol	Details of Specimen	Dimensions (mm)
G	Gage Length	19
W	Width	3.0
T	Thickness	2.0
R	Radius of Fillet	4.0
L	Overall Length	75
A	Length of Reduced section	38
B	Length of Grip Section	19
C	Width of Grip Section	10
D	Diameter of Hole for Pin	3.5
E	Edge Distance from Pin	9.0

The creep specimens were tested on the creep testing machine at temperature 550, 600, and 650 °C. For that reason, we have chosen the applied stress values from reference yield stress from uniaxial tensile loading at elevated temperature of 2.25Cr-1Mo steel at 550, 600, and 650 °C are approximately at 350, 291 and 232 MPa respectively [15]. Therefore, applied load tested at 60%, 70%, 80%, and 90% of 2.25Cr-1Mo steel yield stress at tested temperature. For creep tested at 550 °C used stress level of 210, 245, 280, and 315 MPa. Creep tested at 600 °C used stress levels of 175, 204, 232, and 262 MPa. And creep tested at 650 °C used stress levels of 139, 162, 186, and 209 MPa. Totally, 24 conditions of creep test specimens with different temperature and yield stress were investigated. Every single condition was tested over at least 3 iterations.



Fig. 2. Creep test machine and accessories equipment; (1) Furnace chamber, (2) Dead-weight plates and loading pan, (3) Pin-type grips, (4) Extensometer, (5) LVDT, (6) Specimen, (7) Computer, (8) Furnace temperature.

### 3. Results and Discussion

#### 3.1. Accelerated Creep Tests

The creep strain versus elapsed time plots for ER90S-G and ERNiCrMo-3 welded sample tested at temperatures 550, 600, and 650 °C are presented successively in Figs. 3-5. All data show a comparison of the creep curves properties followed by the creep appearances in three steps including the primary, secondary, and tertiary stages. In the primary creep stage, the primary creep rate decreases with increasing strain until the secondary creep stage or steady-state creep, and then the creep rate is constant. In the tertiary creep stage, the creep rate increases due to occurring the cavitation and crack until the specimen ruptures [16, 17]. The elapsed time of creep curves is significantly important on the applied stress and tested temperature because a slower deformation rate occurs when lower stress applies. On the other hand, the accelerated creep failure was obtained a high-stress level [18, 19]. For all-welded specimens, the creep fracture occurred in the vicinity of the heat-affected zone of the specimens.

#### 3.2. Creep Analysis

The steady-state creep rate is the equation relationship of temperature and stress. It can be described by a power-law [17-20] as shown in Eq. (1)

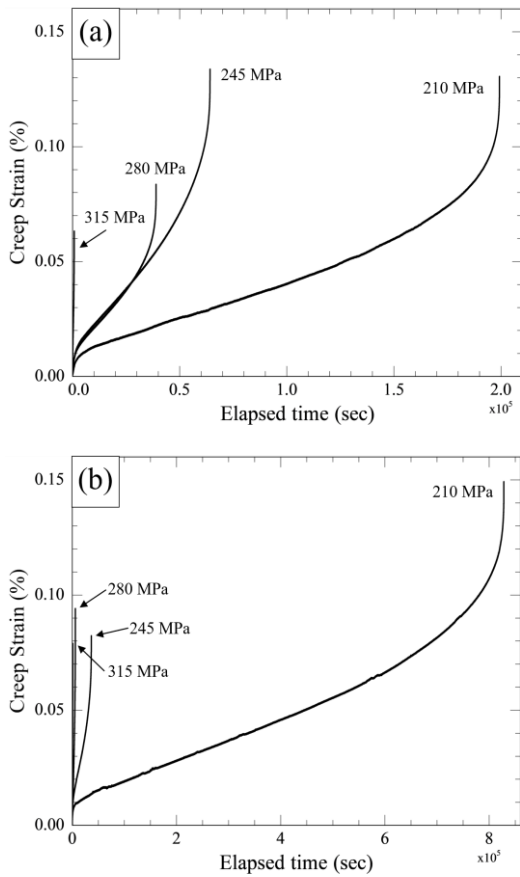


Fig. 3. Creep curves tested at 550 °C of (a) ER90S-G welded and (b) ERNiCrMo-3 welded.

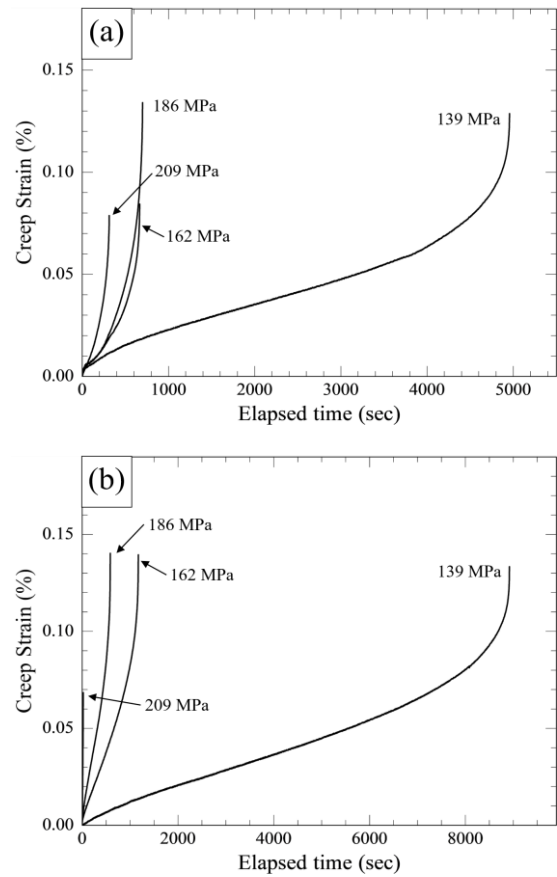


Fig. 5. Creep curves tested at 650 °C of (a) ER90S-G welded and (b) ERNiCrMo-3 welded.

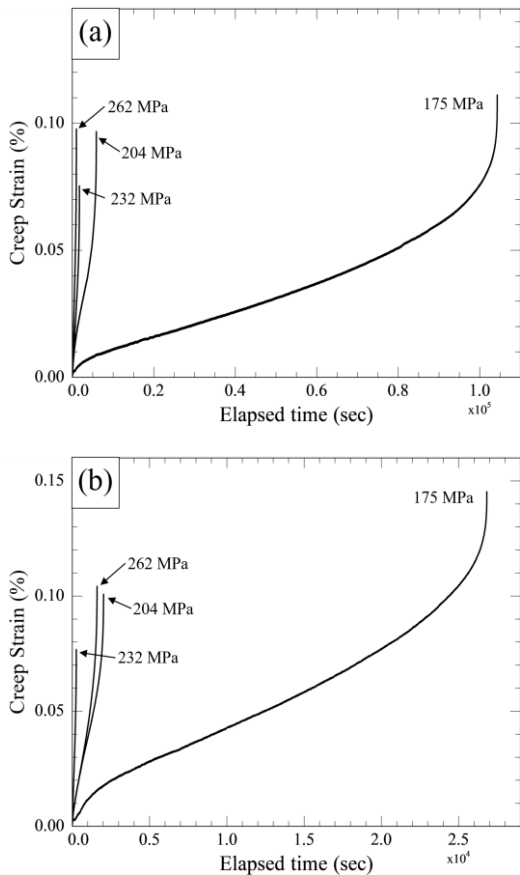


Fig. 4. Creep curves tested at 600 °C of (a) ER90S-G welded and (b) ERNiCrMo-3 welded.

$$\dot{\epsilon}_{ss} = A \cdot \sigma^n \cdot \exp\left(\frac{-Q_c}{R \cdot T}\right) \quad (1)$$

where:  $\dot{\epsilon}_{ss}$  - steady-state creep rate or minimum creep rate

- A - material constant
- $\sigma$  - creep stress, MPa
- $Q_c$  - activation energy for creep, kJ/mol
- R - universal gas constant, J/K·mol
- T - absolute temperature, K
- n - stress exponent

When T constant and  $Q_c$  not varied with stress for reducing Eq. (1) to Eq. (2)

$$\dot{\epsilon}_{ss} = B \cdot \sigma^n \quad (2)$$

where: B - temperature depends on the materials parameter, this is consistent with Norton's law equation.

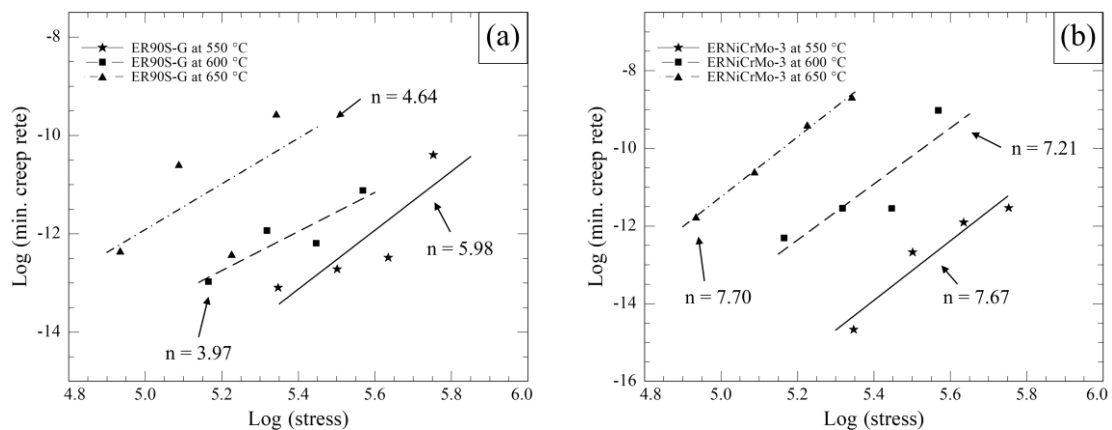
The summary of creep test results on weldments of ER90S-G welded and ERNiCrMo-3 welded are shown in Tables 5 and 6. The minimum creep rate data are plotted versus creep stress on the logarithmic scale shown in Fig. 6 for ER90S-G and ERNiCrMo-3 welded, respectively. The creep properties at elevated temperatures showed that the stress points increase when the tested temperatures for both welded materials increase. The

Table 5. The summary of creep test results on weldments of ER90S-G Welded.

Temperature (°C)	Applied Stress (MPa)	Creep Rate (1/s)	Rupture Time (s)	Stress Exponent ( <i>n</i> )
550	210	2.05x10 <sup>-6</sup>	199,323	5.98
	245	2.99x10 <sup>-6</sup>	64,159	
	280	3.79x10 <sup>-6</sup>	38,996	
	315	3.05x10 <sup>-5</sup>	808	
600	175	2.32x10 <sup>-6</sup>	104,300	3.97
	204	6.56x10 <sup>-6</sup>	5,908	
	232	5.06x10 <sup>-6</sup>	1,755	
	262	1.48x10 <sup>-5</sup>	1,014	
650	139	4.34x10 <sup>-6</sup>	4,957	4.64
	162	2.52x10 <sup>-5</sup>	667	
	186	4.06x10 <sup>-6</sup>	733	
	209	7.03x10 <sup>-5</sup>	314	

Table 6. The summary of creep test results on weldments of ERNiCrMo-3 Welded.

Temperature (°C)	Applied Stress (MPa)	Creep Rate (1/s)	Rupture time (s)	Stress Exponent ( <i>n</i> )
550	210	4.27x10 <sup>-7</sup>	828,120	7.67
	245	3.12x10 <sup>-6</sup>	36,545	
	280	6.73x10 <sup>-6</sup>	5,976	
	315	9.79x10 <sup>-6</sup>	1,137	
600	175	4.52x10 <sup>-6</sup>	26,829	7.21
	204	9.74x10 <sup>-6</sup>	2,022	
	232	9.69x10 <sup>-6</sup>	1,606	
	262	1.21x10 <sup>-4</sup>	261	
650	139	7.78x10 <sup>-6</sup>	9,124	7.70
	162	2.49x10 <sup>-5</sup>	1,173	
	186	8.29x10 <sup>-5</sup>	587	
	209	1.71x10 <sup>-4</sup>	21	

Fig. 6. Plot of  $\ln \dot{\epsilon}_{ss}$  versus  $\ln \sigma$  at temperature 550, 600 and 650 °C for (a) ER90S-G Welded and (b) ERNiCrMo-3 Welded.

values of stress exponent (*n*) can be evaluated from the slope of plotted logarithm fitted Straight line. The *n*-values give information on the creep deformation mechanism, e.g., where *n* = 1, the diffusion mechanism is operative. It defines the grain boundary diffusion mechanism (Nabarro-Herring creep). According to the power-law creep theory, these *n*-values of ER90S-G welded which have been tested at 550, 600, and 650 °C, the *n*-values

obtained *n* = 5.98, 3.97, and 4.64, respectively. These values imply that the dislocation glide and climb-controlled mechanism were operative as the literature indicates that creep occurs in those mechanisms when the values of *n* are approximately 3-5 [16]. However, *n*-values of welded Inconel 625 at 550, 600, and 650 °C obtained were 7.67, 7.21, and 7.70, respectively. These *n*-values imply the occurrence of the power-law breakdown when

$n$ -value  $\geq 9$  approaches. For the most data of 2.25Cr-1Mo, a plot of  $\log \dot{\epsilon}_{ss}$  versus  $\log \sigma$  at different temperatures could be well expressed by straight lines at slope  $n$  value range between 4.5 and 8.5 in the intermediate creep stress region [21-23]. However, we can predict a relevant approximal deformation mechanism of 2.25Cr-1Mo steel under different filler metals in accelerated creep tests conducted as tested conditions.

The correlation of creep data using the Larson-Miller ( $P_{LM}$ ) parameter can be seen in Fig. 7, a plot of applied stress versus the Larson-Miller parameter.

$$P_{LM} = (\log t_r) + C \cdot T \quad (3)$$

where:  $t_r$  - creep rupture life (hr)  
 $C$  - Larson-Miller constant  
 $T$  - absolute temperature (K)

A value of  $C \approx 20$  was initially constantly assumed for 2.25Cr-1Mo steel [21-25]. Where using constant 20 with creep tested of ER90S-G welded and ERNiCrMo-3 welded are linearly plotted Larson-Miller parameter and these obtained R-square ( $R^2$ ) is 0.7766 and 0.7015, respectively. However, the suitable value of the Larson-Miller constant for ER90S-G welded is 30.8 and this value obtained that  $R^2$  is 0.9265, in the same way, the suitable value of the Larson-Miller constant for ERNiCrMo-3 welded is 31.5 and  $R^2$  is 0.9415 in the linear regression analysis.

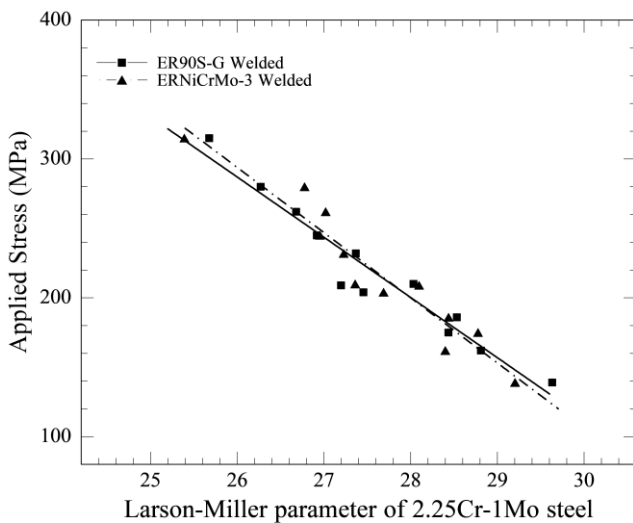


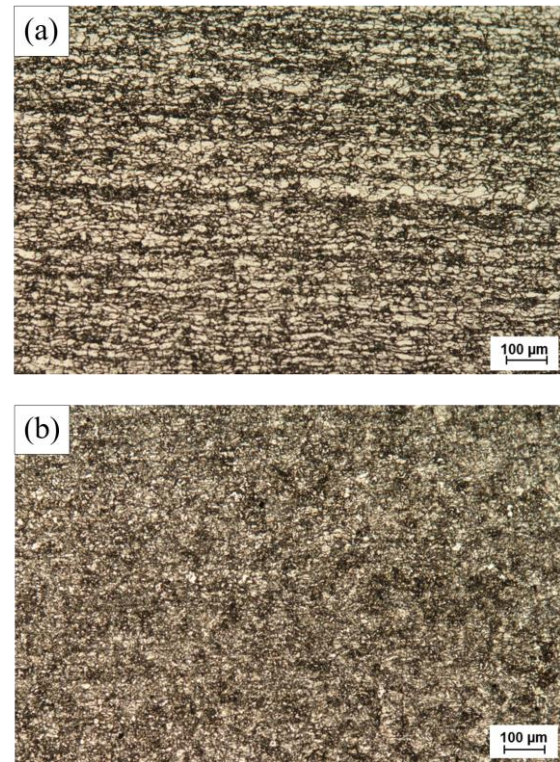
Fig. 7. Applied stress versus Larson-Miller parameter plot of 2.25Cr-1Mo steel joints using ER90S-G and ERNiCrMo-3 filler metals.

Figure 7 shows a plot of applied stress versus the Larson-Miller parameter for tested temperature and actual rupture time at any applied stress to Eq. (3). This shows the small parameter region from accelerated creep can be fitted by a single line of each of the difference filler metals. Normally, the Larson-Miller constant is approximately 20 for carbon and low-alloy steel but the Larson-Miller constant is approximately 30 for high chromium steel [26]. However, the accelerated creep has been tested in a limited applied stress and temperature range. Therefore, the

Larson-Miller constant is approximately 30 for this research. The plotted linear of ER90S-G welded and ERNiCrMo-3 are similar in the applied stress range 139 to 315 MPa. However, when creep tested in narrow stress and temperature range, the constant value is not close to 20 [27]. Other than that, it was found that the linear plotted Larson Miller-parameter both of ER90S-G welded and ERNiCrMo-3 welded were significantly similar because fracture failure occurred at the same location of creep tested specimen of 2.25Cr-1Mo steel welded.

### 3.3. Microstructural Observations

The microstructure of 2.25Cr-1Mo steel before creep testing is presented in Fig. 8. In Fig. 8(a) the microstructure 2.25Cr-1Mo base metal after PWHT condition composed of ferrite in the white region and pearlite in the dark region can be seen. Fig. 8(b) shows the HAZ microstructure of 2.25Cr-1Mo after PWHT condition composed of tempered bainite due to the effect of heating phase transformation during PWHT [28].



Figs. 8. Optical micrographs of 2.25Cr-Mo Steel was applied PWHT before creep tested: (a) Base Metal, (b) Heat Affected Zone.

After creep failure, the fracture surface of each tested specimen was examined by optical fractography and scanning electron microscopy (SEM) fractography. Figure 9 shows optical fractography of longitudinal sections welded creep specimens of ER90S-G and ERNiCrMo-3 tested at the stress level of 175 MPa at 600 °C. The fracture location significant fracture specimens occurred in intercritical region of the heat-affected zone (ICHAZ) due to intercritical region had occurred between  $A_{c1}$  and  $A_{c3}$ . Ferrite phase reverses to austenite in partial during

heating. At the grain boundaries of martensite lath and austenite, the nucleation of fresh austenite is occurred, while the other microstructure is tempered. [29]. That is decreased strength with carbide formation of precipitations and micro void could lead to creep failure.

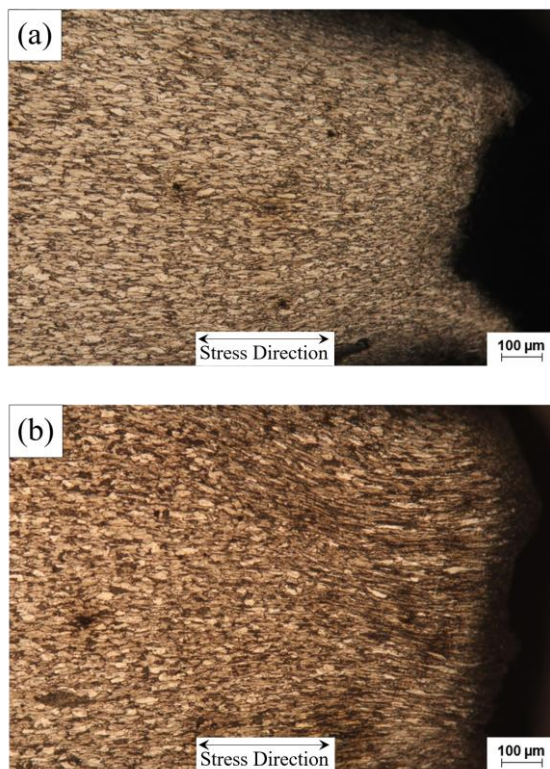


Fig. 9. Optical fractography of the cross-section area after creep tested at temperature 600 °C and applied stress of 175 MPa; (a) ER90S-G welded and (b) ERNiCrMo-3 welded.

Figure 10 shows the SEM fractography of the specimen tested in longitudinal sections of ER90S-G and ERNiCrMo-3 welded at the stress level of 175 MPa and temperature 600 °C. They represent the detail of Fig. 9. It was found that the creep cavitation occurred in the same direction according to the applied stress flow in the ICHAZ of creep tested. The type IV cracking failure occurred because of the creep cavitation in ICHAZ in the 2.25Cr-1Mo steel weldment [30].

Figure 11 compares the fracture surface morphologies of ER90S-G welded specimen to ERNiCrMo-3 welded specimen at a stress level of 210 MPa and temperature 550 °C. Both micrographs consist of predominantly dimple rupture along with evident grain boundary and micro-void coalescence in the fibrous matrix of intercritical region of HAZ [30]. During creep under applied load, grain boundaries occurred in the vacancies in parallel to the stress direction [7]. Figure 12 shows a comparison of the fracture surface morphologies of creep-tested specimens between ER90S-G and ERNiCrMo-3 welded at a stress level of 186 MPa and temperature 650 °C. Characteristics of both micrographs are similar to Fig. 10. It was seen that the tested temperature ranges from 550 °C to 650 °C for both creep

specimens did not influence the fracture surface configurations.

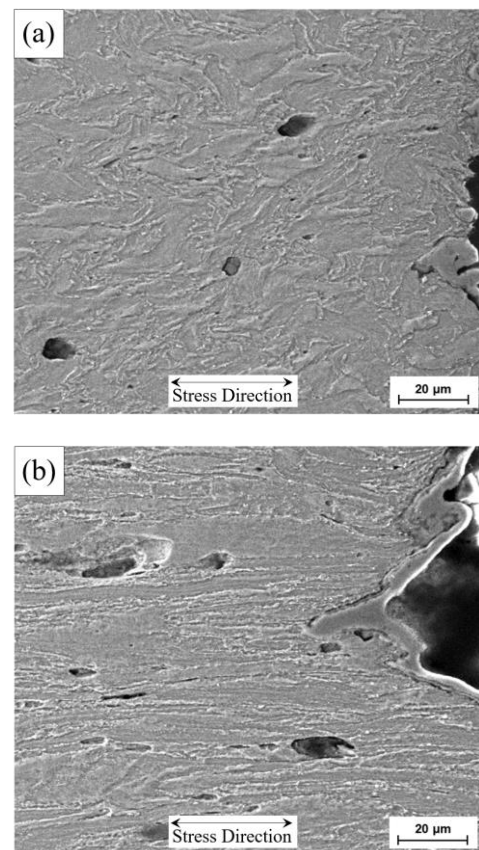


Fig. 10. SEM fractography of the cross-section area after creep tested at temperature 600 °C and applied stress of 175 MPa: (a) ER90S-G welded and (b) ERNiCrMo-3 welded.

#### 4. Conclusions

This research focused on the creep properties and prediction of service life between ER90S-G and ERNiCrMo-3 welded with post-weld heat treatment condition on 2.25Cr-1Mo steel. The summarizes of the results is explained below:

1. The creep service life of tested samples using ER90S-G and ERNiCrMo-3 welded at various applied stresses and temperatures using the Larson-Miller parameter ( $P_{LM}$ ) are quite similar.

2. The creep at elevated temperatures mechanism of ER90S-G welded samples showed the dominance of dislocation creep, but ERNiCrMo-3 welded samples gave values implying the occurrence of nearest power-law breakdown and its values are more than ER90S-G welded during creep tests.

3. The failure of creep tested in both welded samples occurred in the ICHAZ region on the 2.25Cr-Mo base metal at 550, 600 and 650 °C.

4. The ductile fracture modes were found on both of ER90S-G welded sample and ERNiCrMo-3 welded sample, which were analyzed by the dimple morphology. On the other hand, the micro-void sizes of creep exhibited at higher temperature had increased.

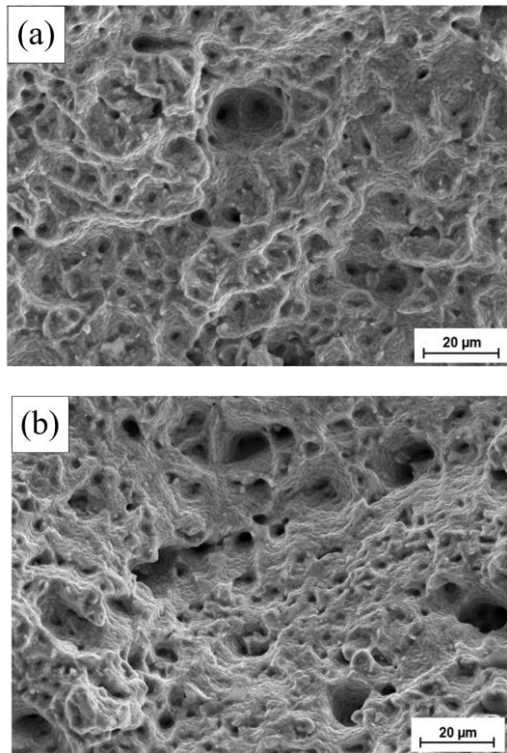


Fig. 11. SEM Fractography of the failure surfaces tested at temperature 550 °C and applied stress of 210 MPa (a) ER90S-G welded and (b) ERNiCrMo-3 welded.

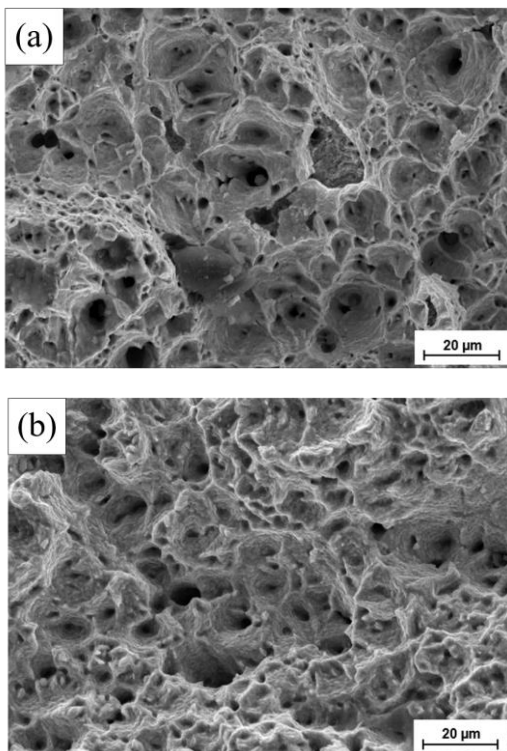


Fig. 12. SEM Fractography of the failure surfaces tested at temperature 650 °C and applied stress of 186 MPa (a) ER90S-G welded and (b) ERNiCrMo-3 welded.

### Acknowledgement

This study was supported by Department of Mining and Materials Engineering, Faculty of Engineering, Prince of Songkla University for research equipment and facilities. The authors would like to thank the Graduate School Scholarship and Center of Excellence in Metal and Materials Engineering (CEMME), Faculty of Engineering, Prince of Songkla University for research funding.

### References

- [1] S. H. Song, J. Wu, X. J. Wei, D. Kumar, S. J. Liu, and L. Q. Weng, "Creep property evaluation of a 2.25 Cr-1Mo low alloy steel," *Mater. Sci. Eng. A*, vol. 527, no. 9, pp. 2398-2403, Apr. 2010.
- [2] W. F. Lima, G. Rigueira, H. C. Furtado, M. B. Lisboa, and L. H. D. Almeida, "Microstructure evolution and creep properties of 2.25 Cr-1Mo ferrite-pearlite and ferrite-bainite steels after exposure to elevated temperatures," *Mat. Res.*, vol. 20, no. 2, pp. 418-422, Mar-Apr. 2017.
- [3] A. Thong-On and C. Boonruang, "Design of boiler welding for improvement of lifetime and cost control," *Mater. Basel Switz.*, vol. 9, no. 11, Nov. 2016.
- [4] A. R. Fernández Fuentes and N. G. Alcántara, "Analysis of the creep behavior and microstructure of PWHT steam piping exposed to service," *Mater. Sci. Eng. A*, vol. 371, no. 1, pp. 127-134, Apr. 2004.
- [5] M. Saga, S. Iwasaki, Y. Tsurusaki, and S. Hata, "Repair technologies of mechanical drive steam turbines for catastrophic damage," in *Proceedings of the 34th Turbomachinery Symposium*, Texas, USA, 2005, pp. 15-24.
- [6] G. A. Webster, R. A. Ainsworth, *High Temperature Component Life Assessment*, 1st ed. UK: Springer Science & Business Media, 1994.
- [7] K. Chen, Y. Xu, and S. Song, "Effect of impurity antimony on the creep behavior of 2.25 Cr-1Mo heat-resistant steel," *Results Phys.*, vol. 13, p. 102208, Jun. 2019.
- [8] V. Shankar, K. Bhanu Sankara Rao, and S. L. Mannan, "Microstructure and mechanical properties of Inconel 625 superalloy," *J. Nucl. Mater.*, vol. 288, no. 2-3, pp. 222-232, Feb. 2001.
- [9] M. J. Donachie and S. J. Donachie, *Superalloys: A Technical Guide*, 2nd ed. Materials Park, OH: ASM International, 2002.
- [10] N. Tammasophon, W. Homkrajai, and G. Lothongkum, "Effect of postweld heat treatment on microstructures and hardness of dissimilar TIG weldment between P22 and P91 steels with Inconel 625 filler metal," *J. Met. Mater. Miner.*, vol. 21, pp. 2011, Jan. 2011.
- [11] *Standard Specification for Seamless Ferritic and Austenitic Alloy-Steel Boiler, Superheater, and Heat-Exchanger Tubes*, ASTM A213/A213M-10, ASTM International, West Conshohocken, PA, 2010.
- [12] Kobe Steel Ltd., *Kobelco Welding Handbook*. [Online]. Available: <https://www.kobelco.co.jp/english/welding/files/handbook.pdf> (accessed July 10, 2020).

- [13] *Specification for Nickel and Nickel-Alloy Bare Welding Electrodes And Rods*, AWS A5. 14/A5. 14M:2011, American Welding Society, US, 2011.
- [14] *Standard Test Methods for Tension Testing of Metallic Materials*, ASTM E8/E8M-13, ASTM International, West Conshohocken, PA, 2013.
- [15] K. Sawada et al., "Catalog of NIMS creep data sheets," *Sci. Technol. Adv. Mater.*, vol. 20, no. 1, pp. 1131-1149, Jan. 2020.
- [16] F. Abe, T. U. Kern, and R. Viswanathan, *Creep-Resistant Steels*, 1<sup>st</sup> ed., Abington, CA: Woodhead Publishing Ltd., 2008.
- [17] M. E. Kassner, *Fundamentals of Creep in Metals and Alloys*, 3rd ed. Waltham, MA: Butterworth-Heinemann, 2015.
- [18] L. O. Bueno and J. F. R. Sobrinho, "Correlation between creep and hot tensile behaviour for 2.25 Cr-1Mo steel from 500°C to 700°C part 1: An assessment according to usual relations involving stress, temperature, strain rate and rupture time," *Matéria (Rio J.)*, vol. 17, no. 3, pp. 1098-1108, Jul. 2012.
- [19] G. E. Dieter, *Mechanical Metallurgy*, 3rd ed. US: McGraw-Hill, 1988.
- [20] R. W. Evans and B. Wilshire, *Introduction to Creep*. London, UK: Institute of Materials, 1993.
- [21] L. de Oliveira Bueno, "Creep Behaviour of 2.25 Cr-1Mo steel-An equivalence between hot tensile and creep testing data," in *ECCC Creep Conference*, London, UK, 2005, pp. 969-980.
- [22] M. T. Whittaker and B. Wilshire, "Advanced procedures for long-term creep data prediction for 2.25 chromium steels," *Metall. Mater. Trans. A*, vol. 44, no. 1, pp. 136-153, Jan. 2013.
- [23] K. Laha, K. Chandravathi, K. Bhanu Sankara Rao, S. L. Mannan, and D. H. Sastry, "A comparison of creep rupture behaviour of 2.25Cr-1Mo and 9Cr-1Mo steels and their weld joints," *High Temp. Mater. Process.*, vol. 19, no. 2, pp. 141-150, Mar. 2000.
- [24] S. Fujibayashi, M. Miura, and K. Togashi, "Life prediction of low alloy ferritic steels based upon the tertiary creep behavior," *ISIJ Int.*, vol. 44, no. 5, pp. 919-926, Jan. 2004.
- [25] S. Fujibayashi, K. Kawano, T. Komamura, and T. Sugimura, "Creep behavior of 2.25Cr1Mo steel shield metal arc weldment," *ISIJ Int.*, vol. 44, no. 3 pp. 581-590, Jan. 2004.
- [26] M. Tamura, F. Abe, K. Shiba, H. Sakasegawa, and H. Tanigawa, "Larson-Miller constant of heat-resistant steel," *Metall. Mater. Trans. A*, vol. 44, no. 6, pp. 2645-2661, Jun. 2013.
- [27] K. Maruyama, F. Abe, H. Sato, J. Shimojo, N. Sekido, and K. Yoshimi, "On the physical basis of a Larson-Miller constant of 20," *Int. J. Press. Vessels Pip.*, vol. 159, pp. 93-100, Jan. 2018.
- [28] D. H. Kang and H. W. Lee, "Microstructure and hardness change in high temperature service depending on Mo content in 2.25Cr-1Mo steel weld metals," *Met. Mater. Int.*, vol. 17, no. 6, pp. 963-967, Dec. 2011.
- [29] J. A. Francis, W. Mazur, and H. K. D. H. Bhadeshia, "Review type IV cracking in ferritic power plant steels," *Mater. Sci. Technol.*, vol. 22, no. 12, pp. 1387-1395, Dec. 2006.
- [30] S. Goyal, K. Laha, K. S. Chandravathi, P. Parameswaran, and M. D. Mathew, "Finite element analysis of type IV cracking in 2.25Cr-1Mo steel weldment based on micro-mechanistic approach," *Philos. Mag.*, vol. 91, no. 23, pp. 3128-3154, Aug. 2011.



**Buntoeng Srikarun** graduated with a bachelor's degree in Mechanical Engineering from Prince of Songkla University in 2012 and M.Eng. in Materials Engineering from Prince of Songkla University in 2015 and Ph.D. in Materials Engineering from Prince of Songkla University in 2019.

I have been appointed as a lecturer at the Department of Mechanical and Robotic Engineering, School of Engineering and Technology, Walailak University in 2020. My field of research are welding and joining technologies, development of new method to improve metallurgical and mechanical properties of hard surfacing and surface cladding applications, railway recondition, and steam turbine rotor repair welding.



**Ittiphol Phonpud** received the B.Eng. degree in metallurgical engineering from Suranaree University of Technology, Thailand in 2010. He received B.Sc. in Occupational Health and Safety from Sukhothai Thammathirat Open University in 2020. From 2010 – present, he works in oil & gas construction business as an Engineer. His research project is about metallurgical and mechanical properties in steam turbine rotor material.



**Prapas Muangjunburee** was born in Nakhon Si Thammarat Province, Thailand in 1967. He received the B.Eng. degree in Industrial Engineering from Prince of Songkla University in 1990 and M.Eng. degree in Mechanical Engineering from Nagaoka University of Technology in 1997. He received the Ph.D. degree in Materials Science and Engineering from The University of Liverpool, United Kingdom, in 2005.

In 2005, he was appointed as a lecturer at the Department of Mining and Materials Engineering, Faculty of Engineering, Prince of Songkla University. He has been an Associated Professor since 2020. He is the author and co-author of more than 30 articles. His research interests include welding technology, welding metallurgy and applications, high temperature oxidation, coating technology, railway welding, and steam turbine rotor welding. He is a reviewer for more than 10 academic journals. Dr. Prapas has gotten a license for professional practice in professional engineer level from Council of Engineers.



**Thawatchai Plookphol** received his B.Eng. degree in Mining and Metallurgical Engineering, in 1981 from Prince of Songkla University, Thailand. He received M.Eng degree in Geotechnical Engineering, in 1987 from Asian Institute of Technology, Thailand. He received M.Sc. degree and Ph.D. in Metallurgical Engineering, in 1996 and 2001, respectively from University of Wisconsin-Madison, USA. He has been working at his research interests including metallurgical engineering, powder metallurgy, and mechanical properties.